

Supporting information of

Synthesis of Pyrrolo[3',2':4,5][1,3]diazepino[2,1,7-cd]pyrrolizine Derivative from Dicyanovinylene-bis(*meso*-aryl)dipyrin

Ji-Young Shin*

Department of Molecular and Macromolecular Chemistry, Graduate School of Engineering, Nagoya University, Furo-cho, Chikusa-ku, Nagoya 464-8603, Japan. Fax: 81-52-747-6771; E-mail: jyshin@chembio.nagoya-u.ac.jp

Content

1. NMR spectra of 2 and 3	-----	page 2
2. Mass spectra of 2 and 3	-----	page 7
3. Crystal structures of 4, 2, and 3	-----	page 8
4. Absorption spectra of 2, 3 _{ox} , and 3 _{red} .	-----	page 10

1. NMR spectra of 2 and 3

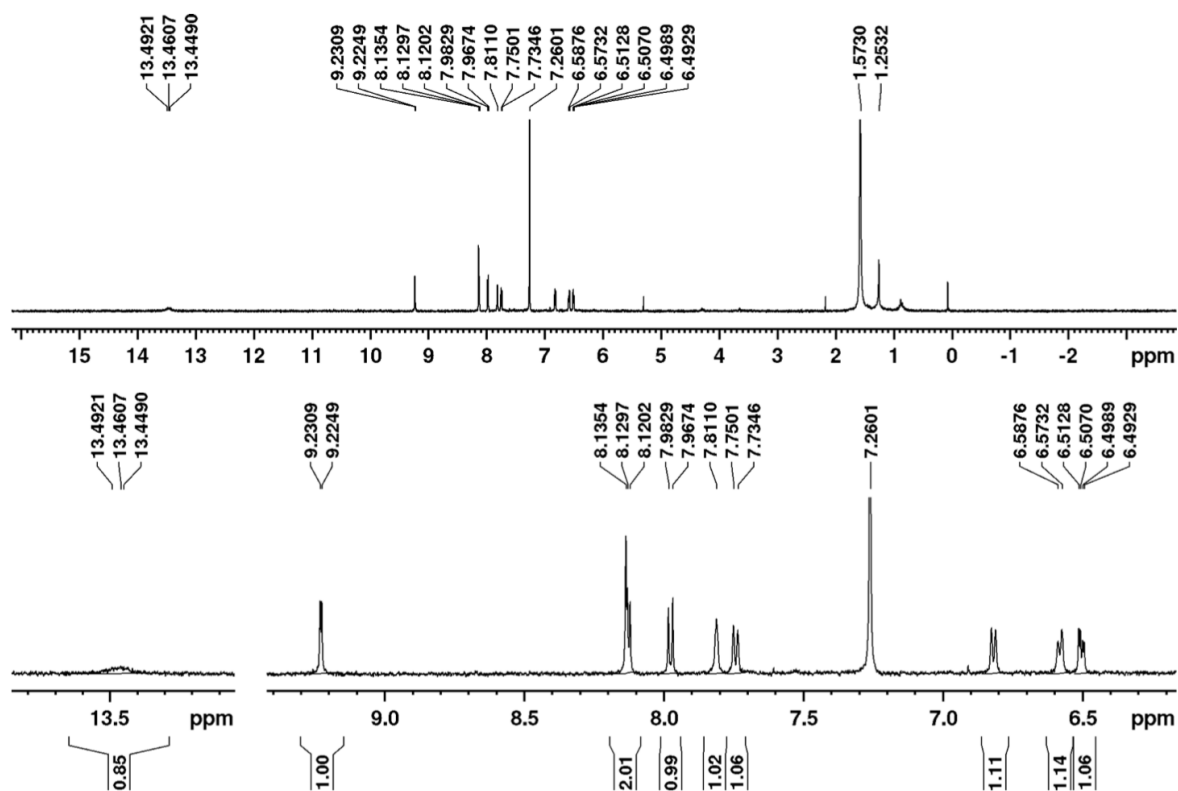


Figure S1. ^1H NMR (300 MHz) spectrum of **3** in CDCl_3 .

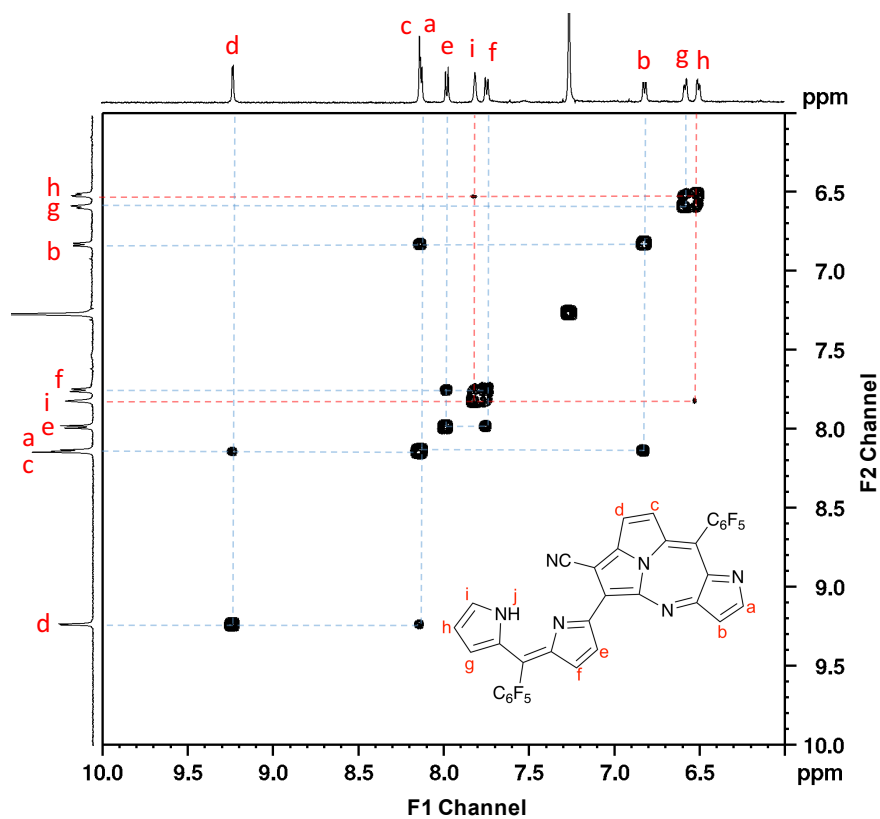


Figure S2. HH COSY ($F_1 = F_2 = 300$ MHz) NMR spectrum of **3** in CDCl_3 .

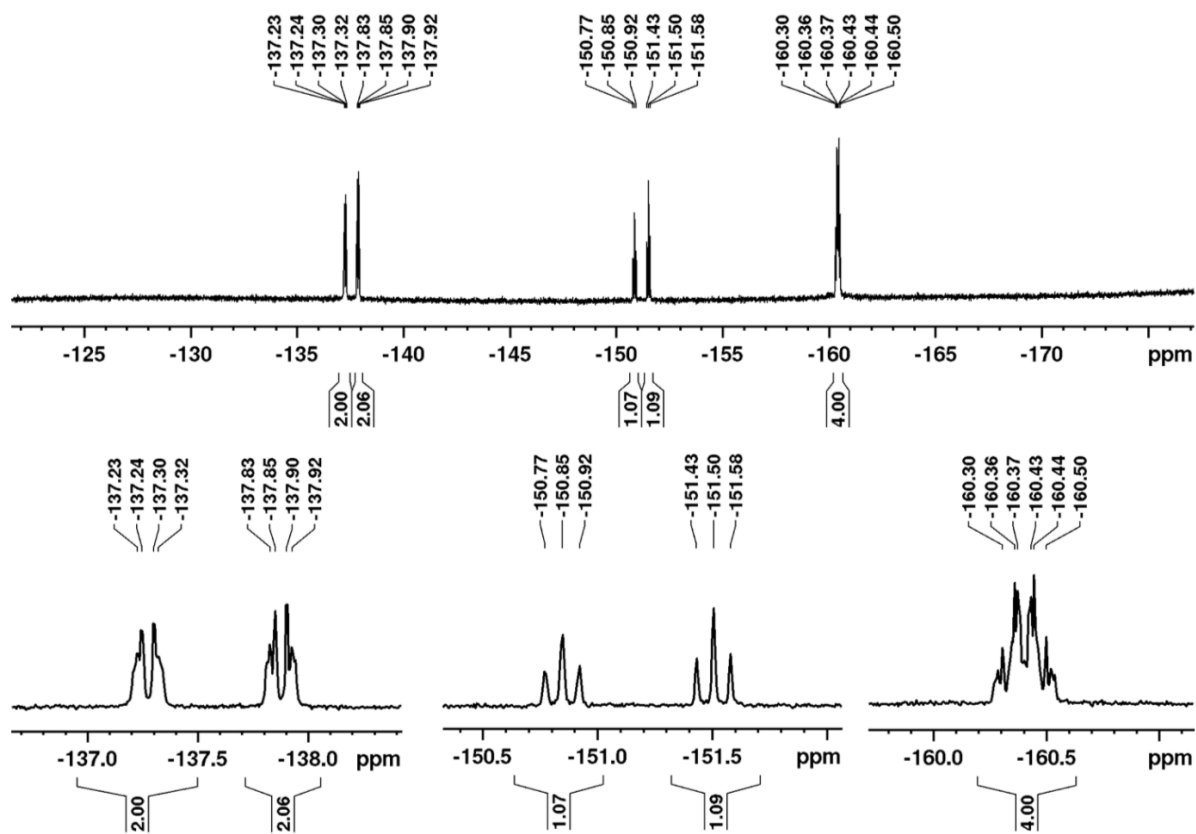


Figure S3. ^{19}F NMR (282.38 MHz) spectrum of **3** in CDCl_3 .

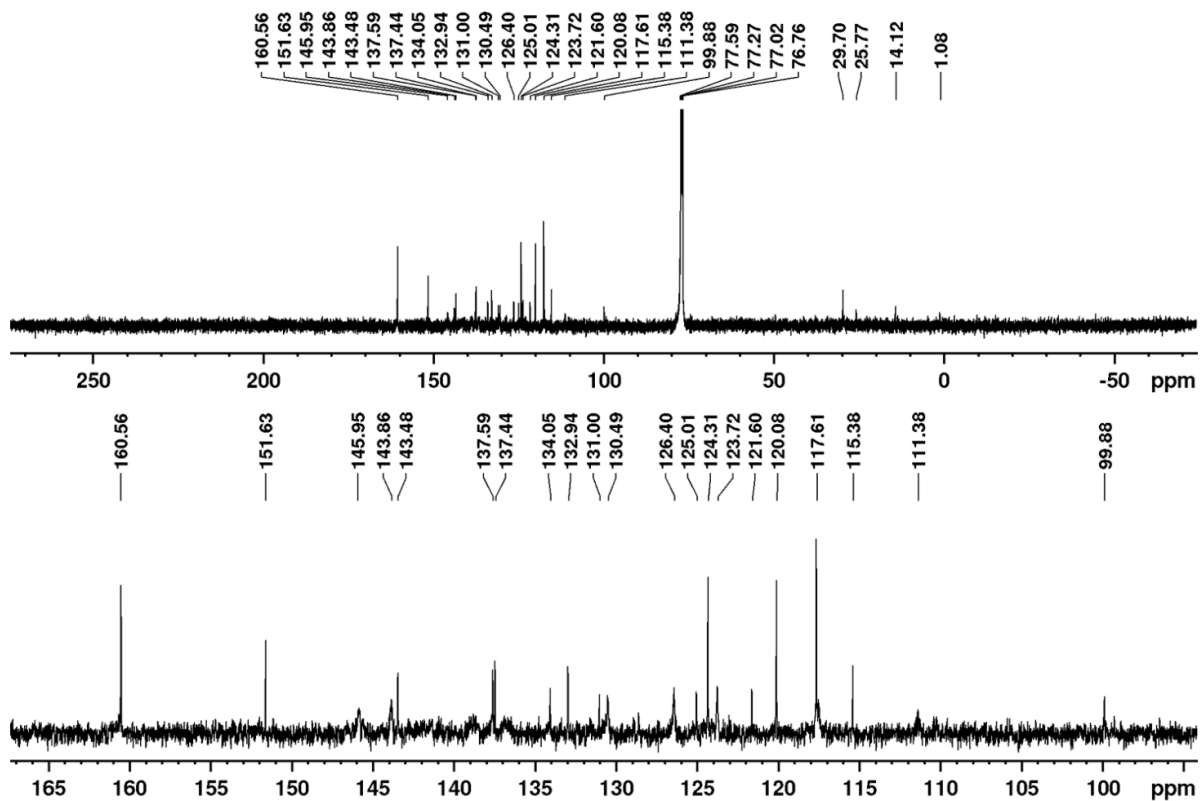


Figure S4. ^{13}C NMR (125.77 MHz) spectrum of **3** in CDCl_3 .

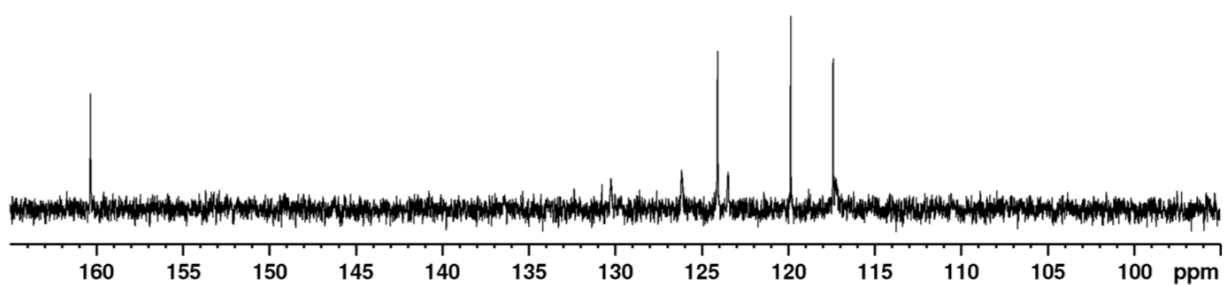
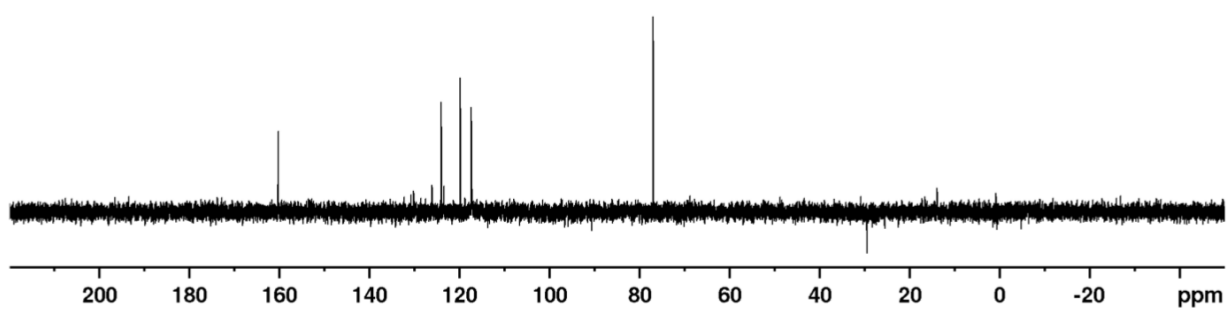


Figure S5. DEPT-135deg NMR (125.77 MHz) spectrum of **3** in CDCl₃.

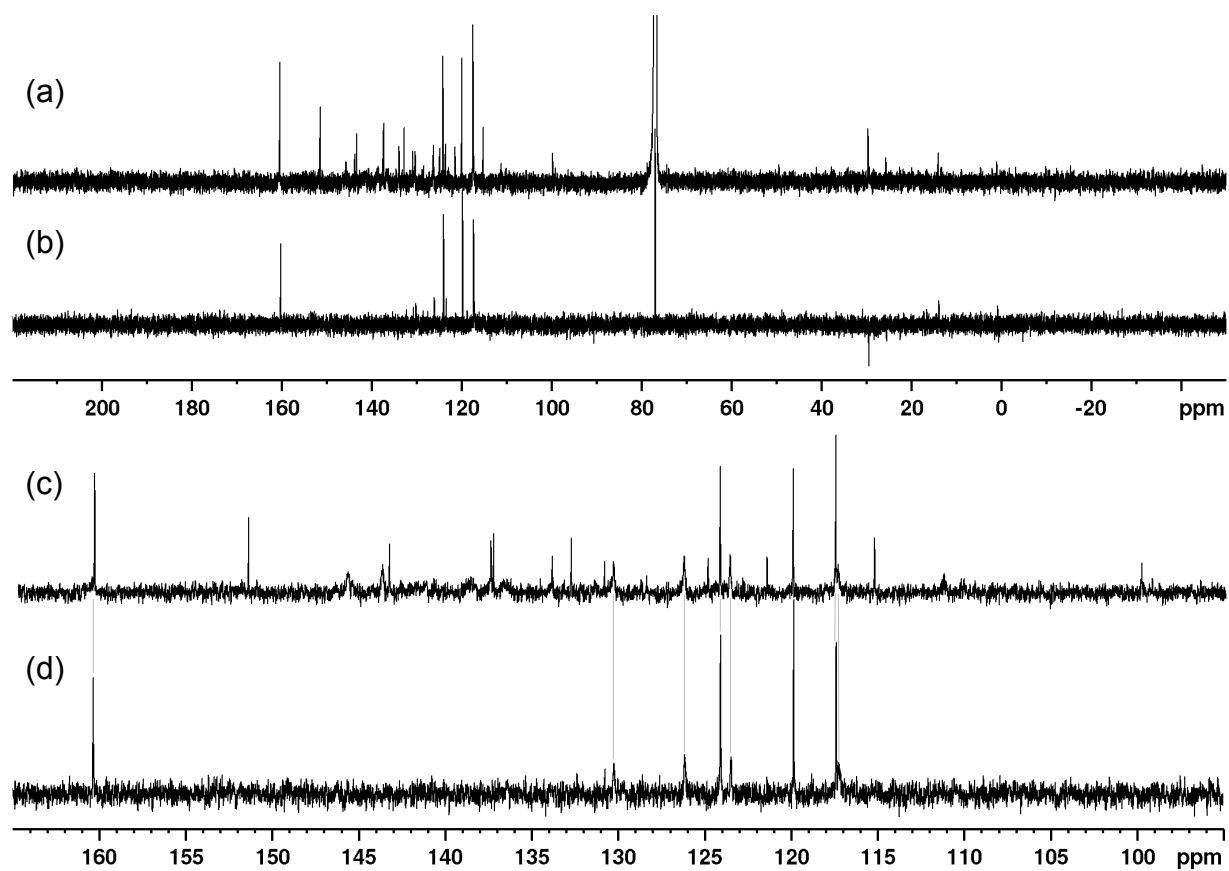


Figure S6. Comparison of carbon peaks between ¹³C (a and c) and DEPT (b and d) NMR (125.77 MHz) spectra of **3** in CDCl₃.

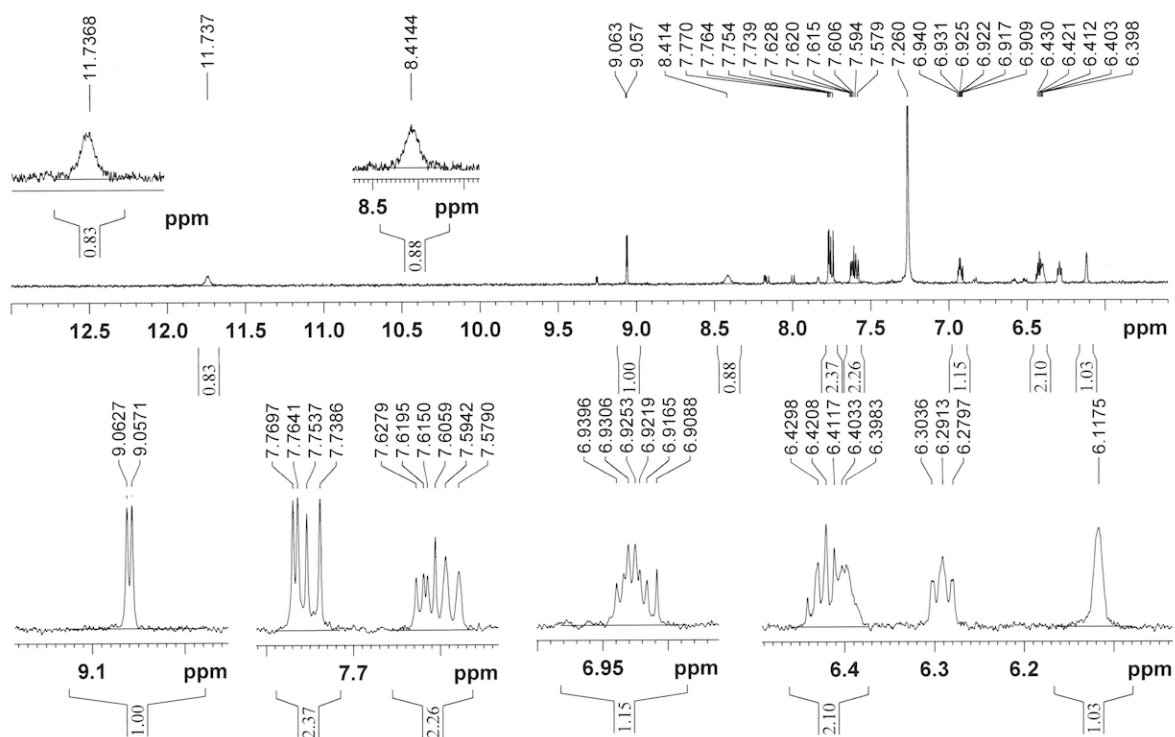


Figure S7. ^1H NMR (300 MHz) spectrum of **2** in CDCl_3 .

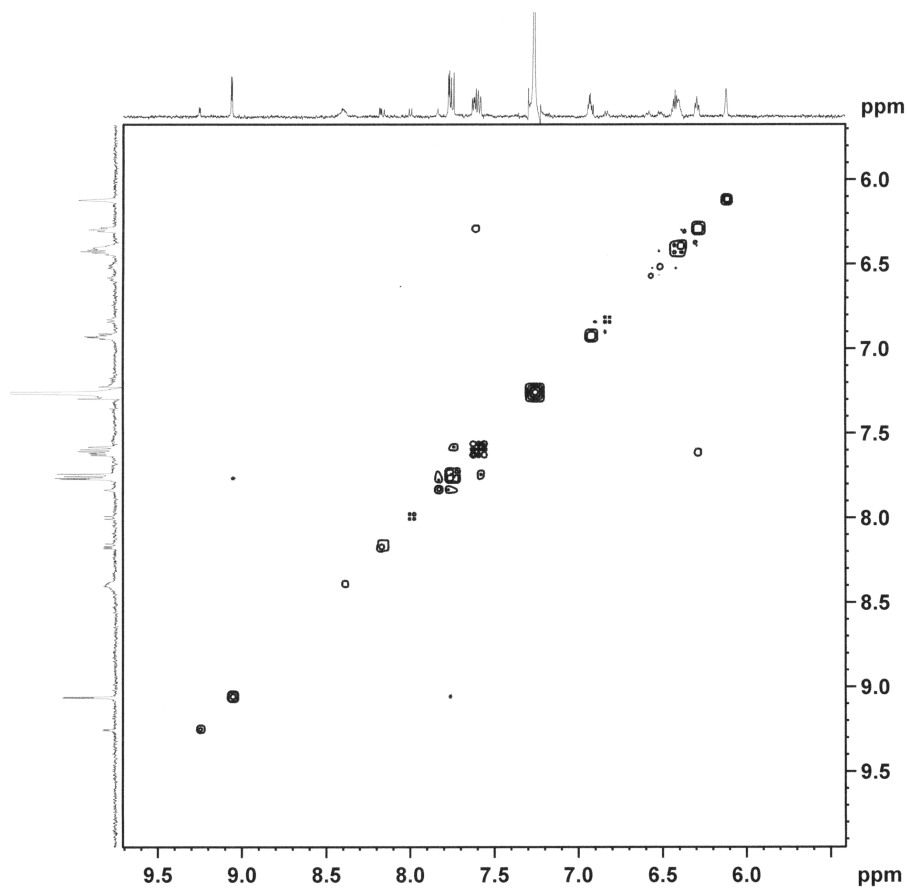


Figure S8. HH COSY ($F_1 = F_2 = 300$ MHz) NMR spectrum of **2** in CDCl_3 .

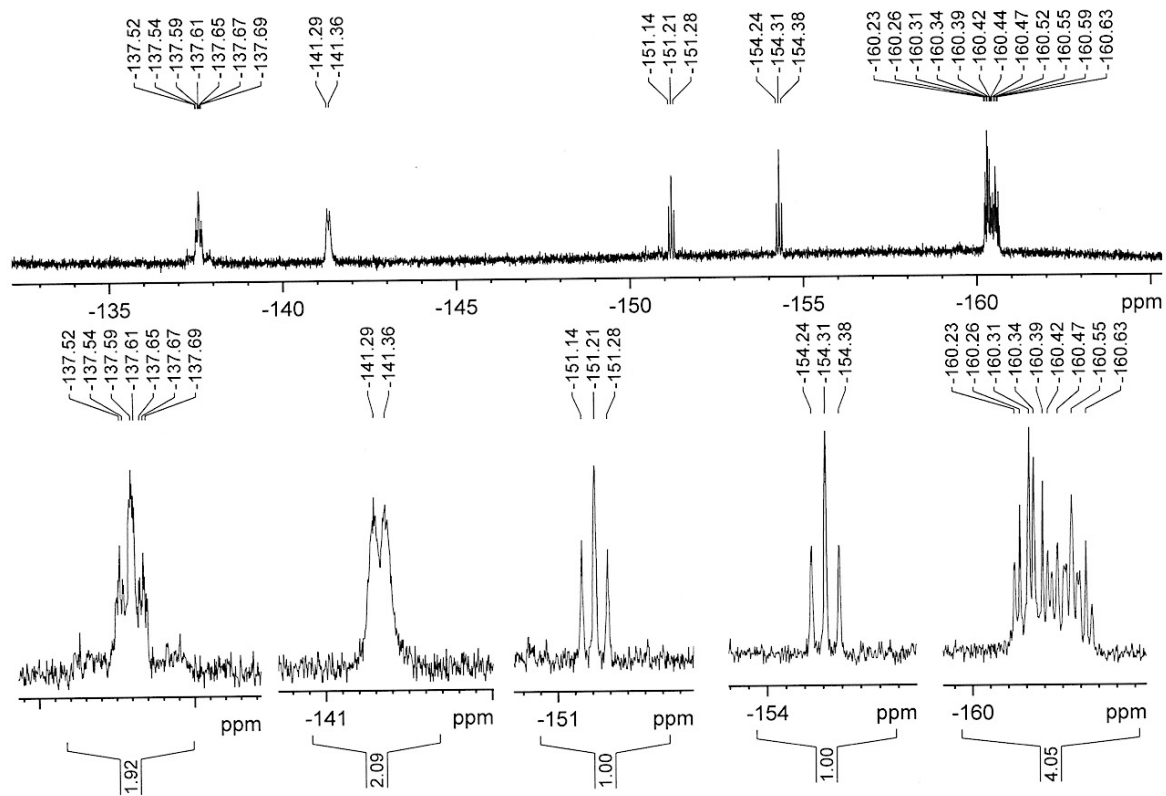


Figure S9. ^{19}F NMR (282.38 MHz) spectrum of **2** in CDCl_3 .

2. Mass spectra of 2 and 3.

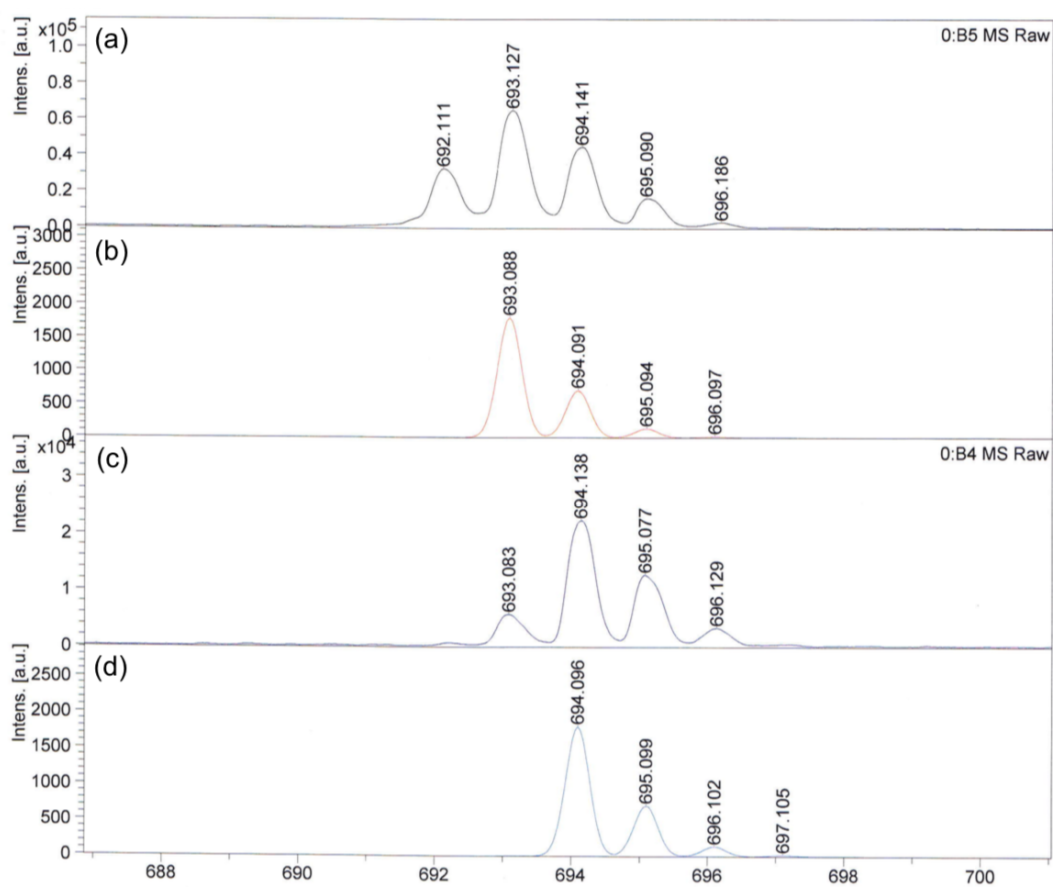


Figure S10. MALDI-TOF mass spectra of **3** (a and b) and **2** (c and d): measured (a and c) and calculated (b and d) masses. (b) and (d) are for $[3 + H]^+$ and $[2]^+$.

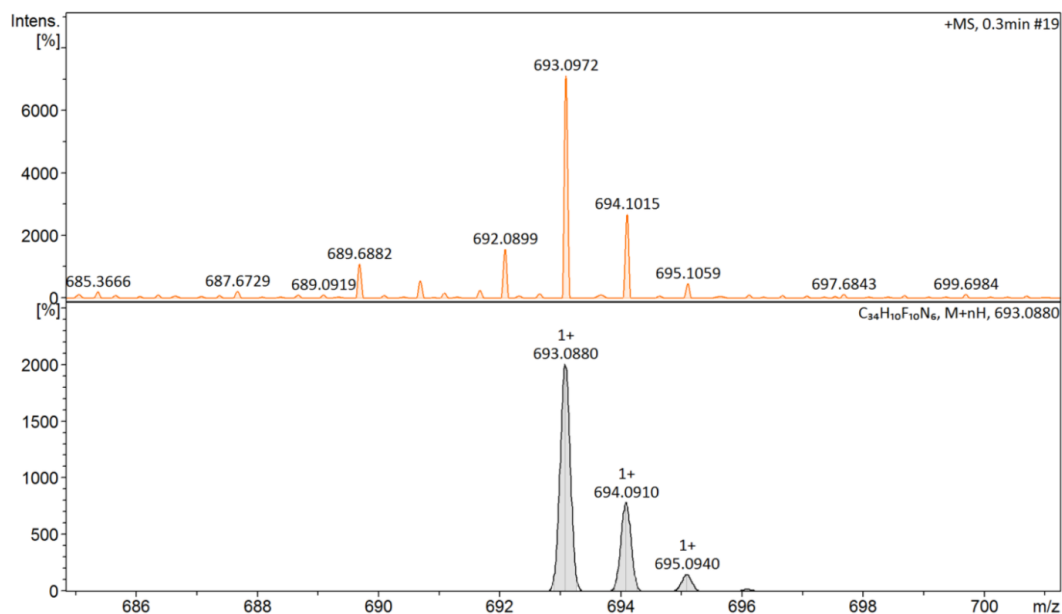


Figure S11. High resolution APCI mass spectrum of **3**.

3. Crystal structures of 4, 2, and 3.

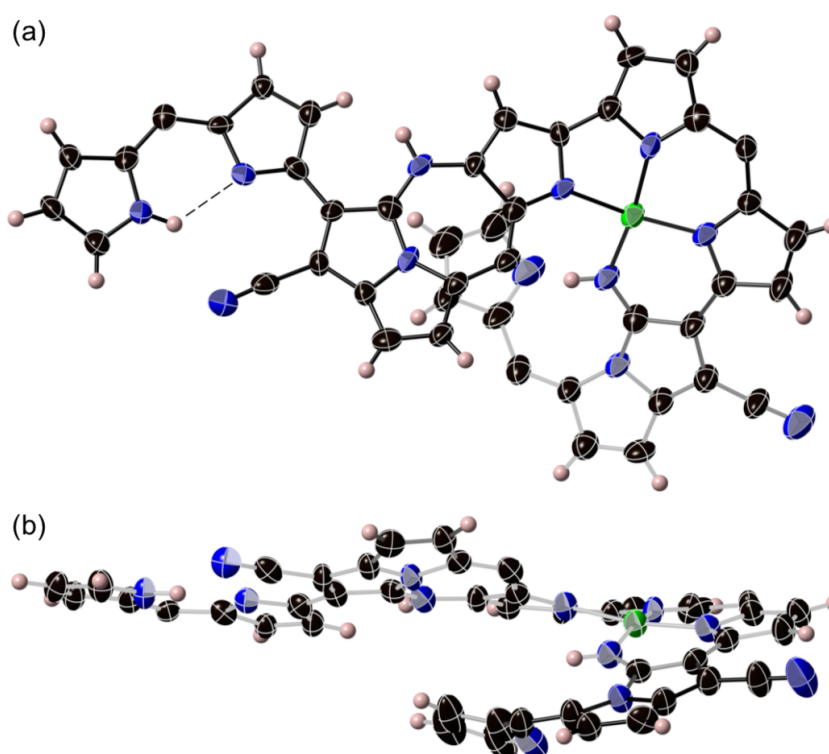


Figure S12. Crystal structure of acyclic Ni^{II} complex **4** (CCDC No. = 1520688): top view (a) and side view (b). *meso*-Pentafluorophenyl groups were omitted for clarity. Thermal ellipsoids are scaled at the 50% probability level. Crystal data of **4**: (C₆₈H₂₀F₂₀N₁₂Ni₂)₂·(N₆Ni₁₄) *M_r* = 2973.51, *T* = 93(2) K, Crystal size = 0.04 x 0.03 x 0.03 mm³, Mo radiation, triclinic, space group *P*-1 (#2), *a* = 16.0744(7) Å, *b* = 16.7126(6) Å, *c* = 26.6119(10) Å, *α* = 105.829(3)°, *β* = 103.161(4)°, *γ* = 97.511(3)°, *V* = 6554.0(5) Å³, *Z* = 2, *P_{calcd.}* = 1.507 g/cm³, *R*₁(*F*) = 0.1124 (*I* > 2(*I*)), *wR*₂(*F*²) = 0.3732 (all), GoF = 1.023, Data completeness = 0.965.

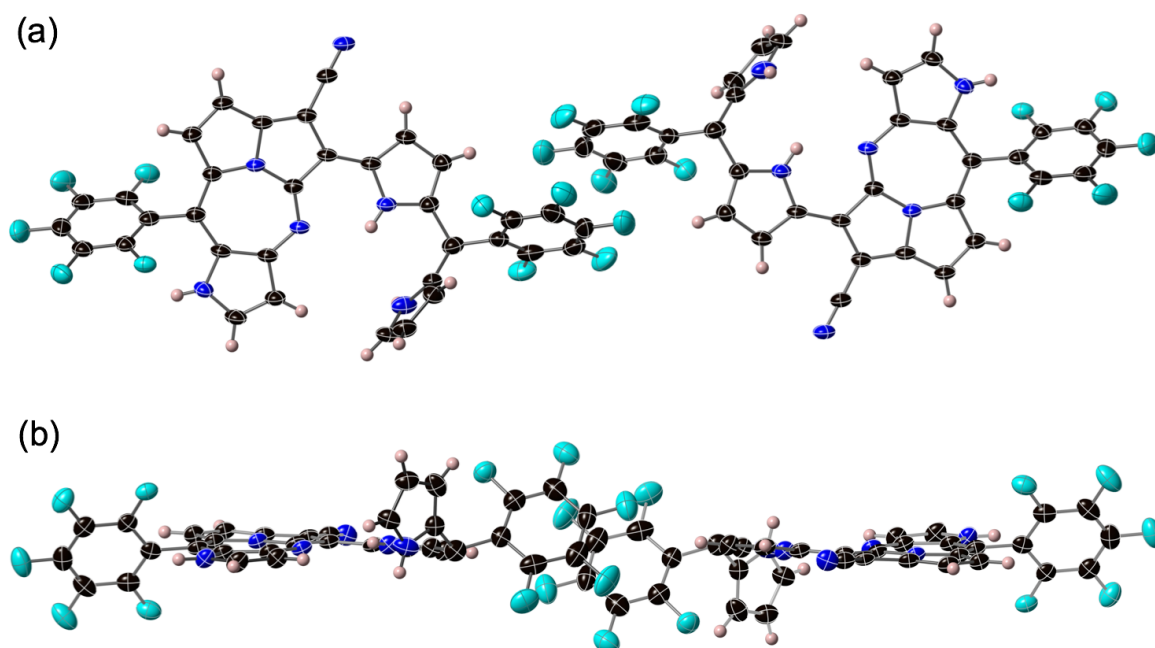


Figure S13. Crystal structure of **2**: top view (a) and side views (b). Thermal ellipsoids are scaled at the 50% probability level.

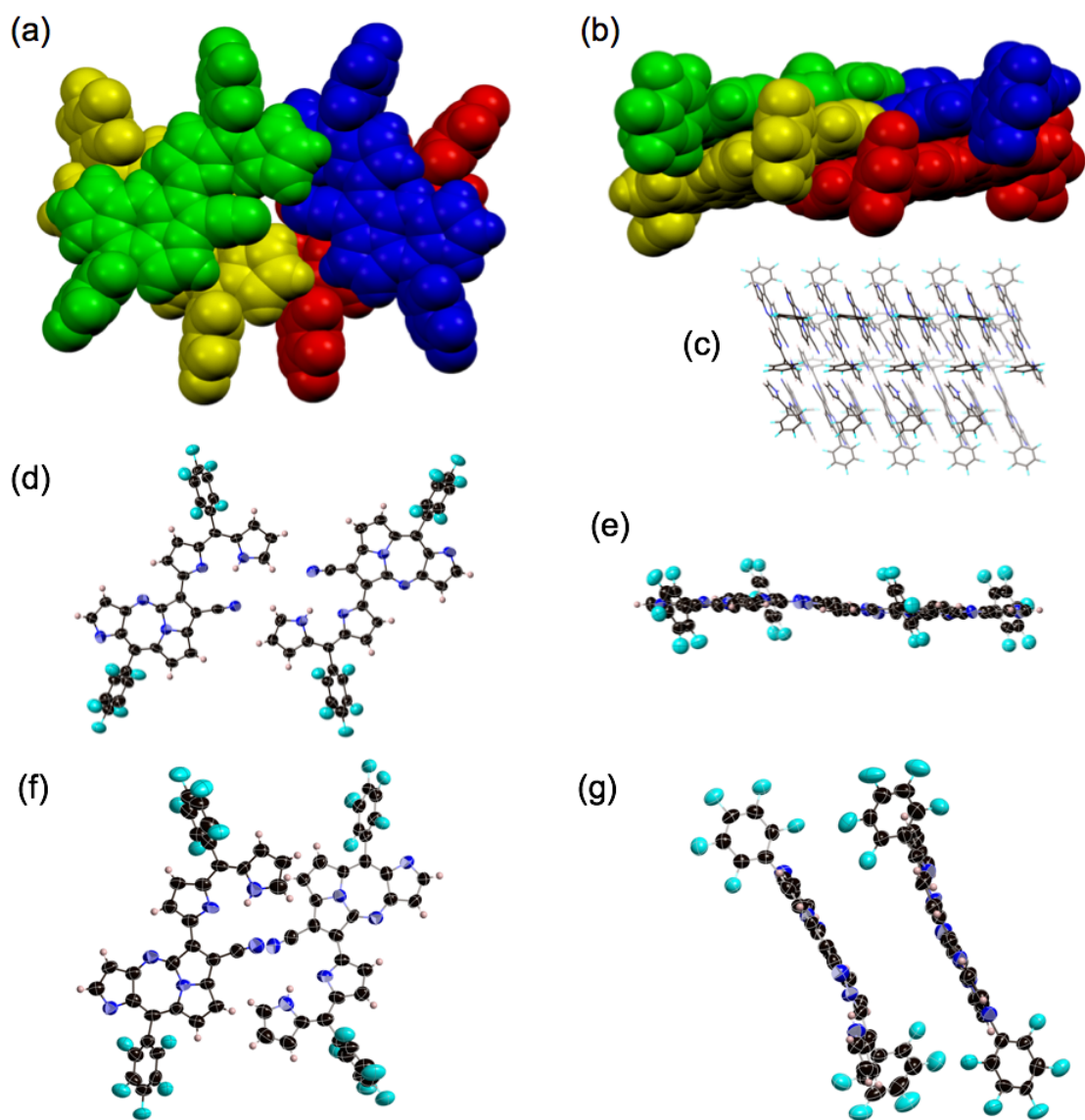


Figure S14. Unit-packing diagrams of **3**: Space-filling structures of top (a) and side (b) views and stick model structure showing a packing pattern. The unit presented a combination of two sets of enantiomers: (d) and (f) are the top view for each of the enantiomers and e and g are their side views, respectively.

4. Absorption spectra of **2**, **3_{ox}**, and **3_{red}**.

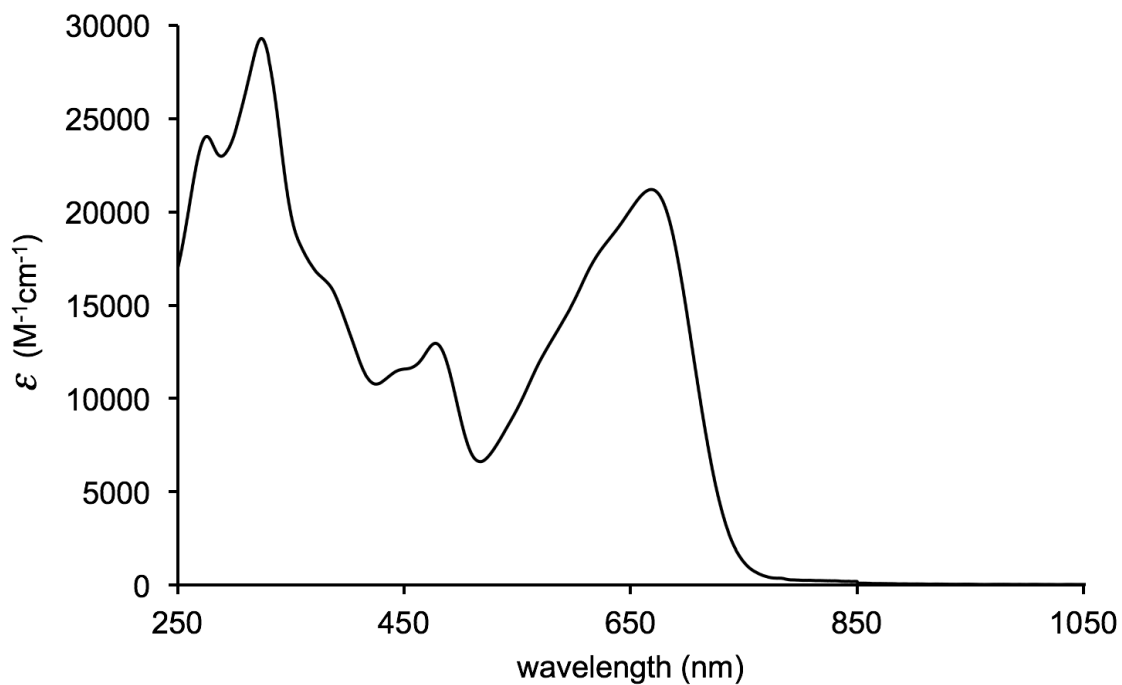


Figure S15. UV Absorption spectrum of **3** in CH_2Cl_2 .

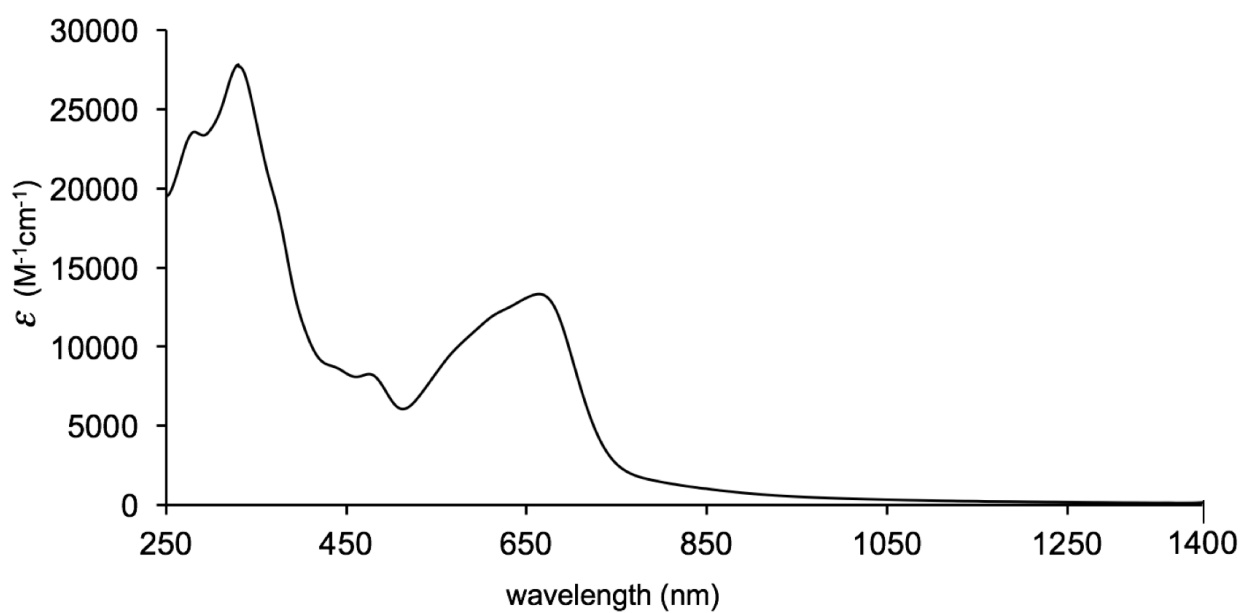


Figure S16. UV Absorption spectrum of **2** in CH_2Cl_2 .

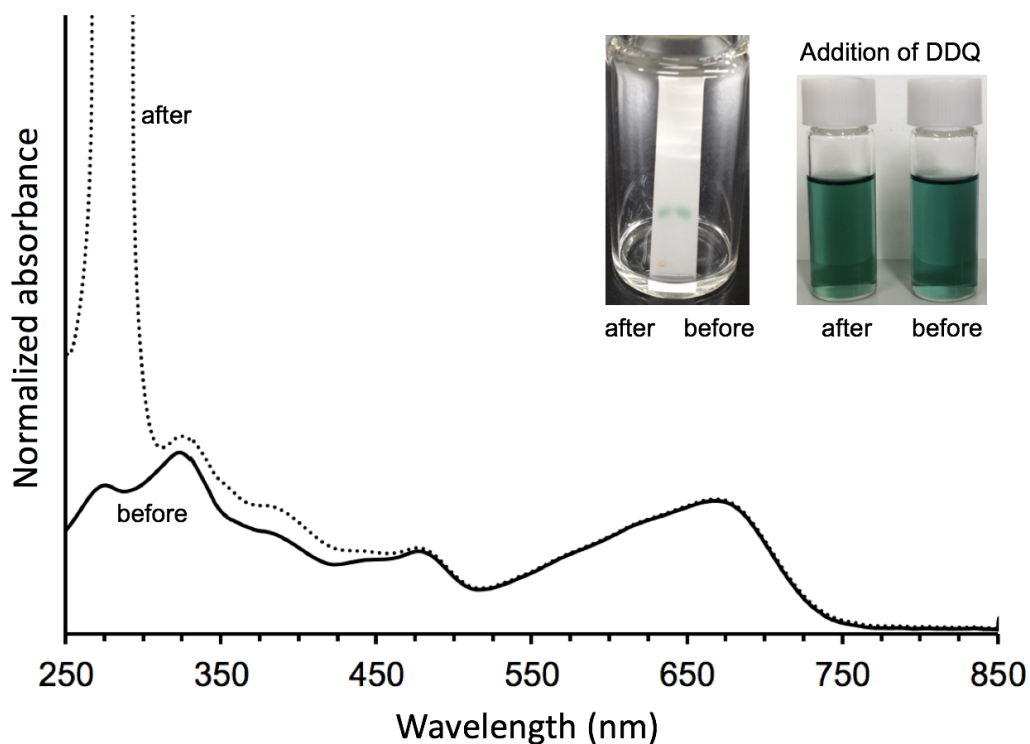


Figure S17. Examine of absorption dependence on a chemical oxidation with DDQ: UV absorption spectra of **3** in CH_2Cl_2 , before (—) and after (·····) addition of excess DDQ. Any significant difference between two samples was observed: The solutions exhibited same green in color as well as exactly same retention time on TLC plate (silica gel with neat CH_2Cl_2).

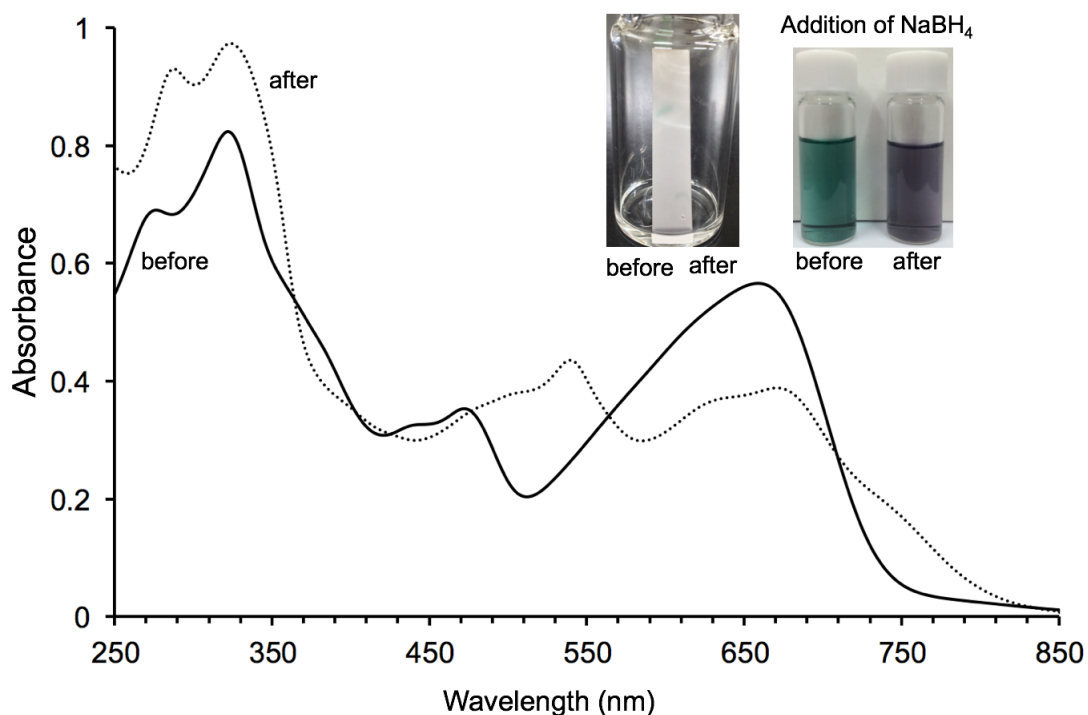


Figure S18. Examine of absorption dependence on a chemical reduction with NaBH_4 : UV absorption spectra of **3** in CH_3OH , before (—) and after (·····) addition of excess NaBH_4 . The initial green was changed to violet in color. Retention time on TLC plate increased with the chemical reduction (silica gel with CH_2Cl_2 including tiny amount of CH_3OH).